

Recombinant BRICHOS chaperone domains delivered to mouse brain parenchyma by focused ultrasound and microbubbles are internalized by hippocampal and cortical neurons



L. Galan-Acosta^a, C. Sierra^{b,1}, A. Leppert^a, A.N. Pouliopoulos^b, N. Kwon^b, R.L. Noel^b, S. Tambaro^a, J. Presto^a, P. Nilsson^a, E.E. Konofagou^{b,c}, J. Johansson^{a,*}

^a Department of Neurobiology, Care Sciences and Society (NVS), Division of Neurogeriatrics, Karolinska Institutet, 141 83 Huddinge, Sweden

^b Ultrasound and Elasticity Imaging Laboratory, Department of Biomedical Engineering, Columbia University, NY, New York, USA

^c Department of Radiology, Columbia University, NY, New York, USA

ARTICLE INFO

Keywords:

BRICHOS
Alzheimer's disease
A β
Focused ultrasound
Blood-brain barrier

ABSTRACT

The BRICHOS domain is found in human precursor proteins associated with cancer, dementia (Bri2) and amyloid lung disease (proSP-C). Recombinant human (rh) proSP-C and Bri2 BRICHOS domains delay amyloid- β peptide (A β) fibril formation and reduce associated toxicity *in vitro* and their overexpression reduces A β neurotoxicity in animal models of Alzheimer's disease. After intravenous administration in wild-type mice, rh Bri2, but not proSP-C, BRICHOS was detected in the brain parenchyma, suggesting that Bri2 BRICHOS selectively bypasses the blood-brain barrier (BBB). Here, our objective was to increase the brain delivery of rh proSP-C (trimer of 18 kDa subunits) and Bri2 BRICHOS (monomer to oligomer of 15 kDa subunits) using focused ultrasound combined with intravenous microbubbles (FUS + MB), which enables targeted and transient opening of the BBB. FUS + MB was targeted to one hemisphere of wild type mice and BBB opening in the hippocampal region was confirmed by magnetic resonance imaging. Two hours after FUS + MB brain histology showed no signs of tissue damage and immunohistochemistry showed abundant delivery to the brain parenchyma in 13 out of 16 cases given 10 mg/kg of proSP-C or Bri2 BRICHOS domains. The Bri2, but not proSP-C BRICHOS domain was detected also in the non-targeted hemisphere. ProSP-C and Bri2 BRICHOS domains were taken up by a subset of neurons in the hippocampus and cortex, and were detected to a minor extent in early endosomes. These results indicate that rh Bri2, but not proSP-C, BRICHOS, can be efficiently delivered into the mouse brain parenchyma and that both BRICHOS domains can be internalized by cell-specific mechanisms.

1. Introduction

Alzheimer's disease (AD) is the most common form of dementia and there is currently no successful disease-modifying treatment available (Winblad et al., 2016). AD is characterized by accumulation of amyloid β -peptide (A β) in plaques and of hyperphosphorylated tau in neurofibrillary tangles. According to the amyloid cascade hypothesis, A β aggregation into neurotoxic oligomers and amyloid fibrils is the main underlying pathogenic mechanism in AD (Finder and Glockshuber, 2007; Hardy and Selkoe, 2002). Thus, many strategies to treat AD focus on preventing A β aggregation and neurotoxicity (Ankarcona et al., 2016).

The BRICHOS domain is a naturally occurring chaperone with anti-amyloid properties (Cohen et al., 2015; Knight et al., 2013). BRICHOS is found in 10 human proprotein families, among them Bri2 (also known as integral membrane protein 2b, ITM2B) and pro-surfactant protein C (proSP-C) (Hedlund et al., 2009; Sanchez-Pulido et al., 2002). BRICHOS containing proteins are implicated in two different amyloid diseases; familial British or Danish dementias (FBD and FDD) in the case of Bri2 (Canton et al., 2015) and interstitial lung disease associated with mutant proSP-C (Nogee et al., 2002; Nogee et al., 2001; Willander et al., 2012). Recombinant human (rh) BRICHOS domains from proSP-C and Bri2 delay A β 40 and A β 42 fibril formation *in vitro* by blocking specific steps in the A β fibrillation pathway (Arosio et al., 2016; Cohen et al.,

Abbreviations: A β , amyloid- β peptide; BBB, blood brain barrier; IF, immunofluorescence; IHC, immunohistochemistry; MRI, magnetic resonance imaging; MB, microbubbles; FUS, focused ultrasound; CNS, central nervous system

* Corresponding author.

E-mail address: janne.johansson@ki.se (J. Johansson).

¹ Communications & PR, Centre for Genomic Regulation, 08003 Barcelona, Spain

<https://doi.org/10.1016/j.mcn.2020.103498>

Received 6 November 2019; Received in revised form 30 April 2020; Accepted 2 May 2020

Available online 08 May 2020

1044-7431/© 2020 The Authors. Published by Elsevier Inc. This is an open access article under the CC BY-NC-ND license (<http://creativecommons.org/licenses/by-nc-nd/4.0/>).

2015), prevent A β 42 induced reduction of γ oscillations in hippocampal slice preparations (Chen et al., 2017; Kurudenkandy et al., 2014), and *in vivo* they improve lifespan and locomotor function in a *Drosophila* fly model of AD (Hermansson et al., 2014; Poska et al., 2016). Based on these results, the BRICHOS domain is interesting for development of novel strategies for AD treatment. A recent study showed that rh Bri2 BRICHOS can pass over the blood-brain barrier (BBB) after peripheral administration in wild type mice, while rh proSP-C BRICHOS only passed into the cerebrospinal fluid (Tambaro et al., 2019). The different abilities of Bri2 and proSP-C BRICHOS to pass the BBB might be linked to their different amino acid sequences, physico-chemical properties, and/or variable range of assembly states: trimer for proSP-C BRICHOS and monomer to oligomers with 20–30 subunits for Bri2 BRICHOS (Willander et al., 2012; Chen et al., 2017). Bri2 is produced in the central nervous system (CNS) as well as in peripheral organs (Baron and Pytel, 2017; Zeisel et al., 2015), while proSP-C is exclusively produced in the alveolar type II cells (Glasser et al., 1990). The amount of Bri2 BRICHOS that is spontaneously delivered over the BBB (about 0.5% of the administered amount) (Tambaro et al., 2019) makes it difficult to further study the fate of the rh Bri2 BRICHOS domain in the CNS. For example, it appeared that some cells in the CNS internalized rh Bri2 BRICHOS that had been administered intravenously (Tambaro et al., 2019), but the identities of the cells or intracellular location of the BRICHOS domain could not be determined.

The BBB functions to maintain a delicate environment required for proper neuronal function, however this also makes it a barrier to drugs targeted to the brain, and most large molecules are unable to spontaneously cross the BBB (Mikitsh and Chacko, 2014). Various methods have been developed to deliver drugs and other compounds over the BBB (Brasnjevic et al., 2009; Mikitsh and Chacko, 2014). Focused ultrasound combined with intravenously administered microbubbles (FUS + MB) is a suitable technology that has been shown in multiple *in vivo* models to efficiently deliver proteins over the BBB and to a specifically targeted brain region in a minimally invasive way (Burgess and Hynynen, 2014; Hynynen et al., 2001; Konofagou, 2012; Lipsman et al., 2018; Sierra et al., 2017; Wu et al., 2014). This technique involves intravenous injection of lipid-based MBs together with the molecules to be delivered (Sierra et al., 2017). The ultrasonic waves make the MBs cavitate within the capillaries in the brain already at low acoustic energy (Tung et al., 2011). At these low pressures, MBs exhibit stable cavitation which induces an increase in the opening of the BBB without causing any vascular damage, making it a safe method (Baseri et al., 2010; Choi et al., 2007a, 2007b; Downs et al., 2015). This makes the tight junctions between the endothelial cells loosen transiently, which results in transient and local opening of the BBB. As a result, macromolecules present in the circulation are delivered efficiently into the brain parenchyma (Chen et al., 2014). The aim of this study was to evaluate the fate of rh Bri2 and proSP-C BRICHOS delivered into the brain of wild type mice by the use of FUS + MB.

2. Materials and methods

2.1. Expression and purification of recombinant proteins

Bri2 BRICHOS domain, corresponding to amino acid residues Bri2 (113–231) of human full-length Bri2 (NP_068839.1) as a fusion protein with His₆, N-terminal solubility tag from spider silk protein (Kronqvist et al., 2017), a thrombin cleavage site and AU1 tag (DTYRYI) added by PCR amplification C-terminally of the BRICHOS domain, was expressed in competent *E. coli* Shuffle T7 cells (Chen et al., 2017; Poska et al., 2016; Tambaro et al., 2019). The cells were incubated at 30 °C in LB medium, supplemented with 15 μ g/mL kanamycin. Protein expression was induced at OD_{600 nm} = 0.6–0.8 by adding 0.5 mM isopropyl β -D-1-thiogalactopyranoside (IPTG). The temperature was lowered to 20 °C and after overnight growth, cells were harvested by 3000 \times g centrifugation at 4 °C. After that, cell pellets were re-suspended in 20 mM

Tris-HCl buffer pH 8.0, and sonicated for 5 min on ice (2 s on, 2 s off, 65% of amplitude). The lysate was centrifuged (24,000 \times g) at 4 °C for 30 min, and the supernatant containing the fusion protein was then poured onto a 2.5 mL IMAC column (Ni Sepharose™ 6 Fast Flow, GE Healthcare) previously equilibrated with 20 mM Tris-HCl pH 8.0. Unbound proteins were washed away and the fusion protein was eluted with 300 mM imidazole. The elute was dialyzed (regenerated cellulose RC, 6–8 kDa membrane; Spectrum Lab) against 20 mM Tris pH 8.0, containing thrombin (Merck) (enzyme/substrate weight ratio of 0.001) to cleave off the His₆-NT-tag during overnight incubation at 4 °C. The proteins were re-applied onto the IMAC column to release the His₆-NT-tag and Bri2 BRICHOS domains were eluted with 20 mM Tris pH 8.0. The purity of the protein was investigated by SDS-PAGE (Supplementary Fig. S1) and protein concentration was determined using an extinction coefficient of 12,045 M⁻¹ cm⁻¹ for A₂₈₀.

Human proSP-C BRICHOS domain (proSP-C residues 59–197) was expressed and purified as previously described (Johansson et al., 2009; Johansson et al., 2006; Willander et al., 2012). Briefly, the construct was expressed in *E. coli* strain Origami 2 (DE3) pLysS (Novagen, Madison, WI) as a fusion protein with thioredoxin-His₆ and then purified using Ni²⁺ column chromatography (Qiagen, Ltd. West Sussex, UK). After cleavage with thrombin (Merck) (enzyme/substrate weight ratio of 0.001) for 16 h, the protein was dialyzed against 20 mM Tris-HCl, 50 mM NaCl, pH 8.0 and applied on another Ni²⁺ column to remove the thioredoxin and His₆-tag. Then, the protein was purified by anion exchange chromatography over a column equilibrated with 20 mM Tris, pH 8.0 (Johansson et al., 2006). The protein concentration was determined by measuring the absorbance at 280 nm and using an extinction coefficient of 9190 M⁻¹ cm⁻¹.

Before injection into mice, rh Bri2 and proSP-C BRICHOS proteins were passed over a PD-10 desalting column (GE Healthcare, UK) and eluted with filtered and autoclaved phosphate buffer saline (PBS), pH 7.4. To remove endotoxins, the proteins were passed over Pierce High-Capacity endotoxin removal columns (Thermo scientific). According to manufacturers instructions, the endotoxin removal column was washed with five bed volumes of 0.2 M NaOH at room temperature before the first use and after each subsequent use. Then it was centrifuged at 500 \times g for 1 min to remove 0.2 M NaOH, and the column was washed three times with five bed volumes of 2 M NaCl and five bed volumes of endotoxin-free ultrapure water. The recombinant proteins were applied to the resin, incubated with end-over-end mixing for 1 h at room temperature and then collected by centrifugation (500 \times g, 1 min) in endotoxin-free tubes. The recombinant proteins were finally passed through a 0.22 μ m Millex-GV filter (Millipore Ltd.), protein concentration were measured, and they were stored at –20 °C in autoclaved tubes and kept frozen until about 30 min before injections to avoid formation of larger species (Chen et al., 2017). SDS-PAGE was performed before and after endotoxin removal (Supplementary Fig. S1).

2.2. Synthesis of microbubbles

Lipid-coated microbubbles were produced and isolated based on a published protocol (Feshitan et al., 2009). Briefly, 90% (mol/mol) 1,2-distearoyl-*sn*-glycero-3-phosphocoline (DSPC) and 10% (mol/mol) 1,2-distearoyl-*sn*-glycero-3-phosphoethanolamine-N-(methoxy(polyethylene glycol)2000) (DSPE-PEG2000) (Avanti Polar Lipids, Alabaster, AL) were dissolved in PBS/glycerol (10% volume)/propylene glycol (10% volume). The lipid mixture was sonicated in order to disperse the lipid aggregates into small, unilamellar liposomes. Perfluorobutane, which acts as a gas core, was introduced in order to activate the microbubbles. Lastly, 4–5 μ m microbubbles were isolated by centrifugation for 10 min at 300 \times g and concentration and size distribution were measured (Feshitan et al., 2009; Vlachos et al., 2010).

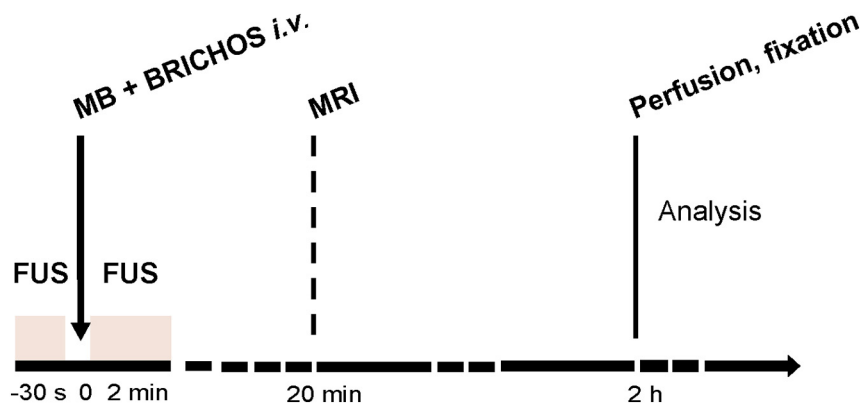


Fig. 1. Experimental overview. For intravenous administration, 1 or 10 mg/kg of rh proSP-C BRICHOS or rh Bri2 BRICHOS-AU1 were injected together with lipid-coated microbubbles (MB) and focused ultrasound (FUS) was applied to the left hippocampus for a total time of 2.5 min. Mice were sacrificed 2 h after BRICHOS administration and brains were embedded in paraffin for histological analysis.

2.3. Animals

Adult female mice (strain: C57BL/6, weight: 20–25 g) were used. Eleven mice were used for rh Bri2 and 9 mice for proSP-C BRICHOS delivery. All mice were kept under controlled conditions of humidity and temperature on a 12 h light-dark cycle. All animal experiments were approved and carried out according to the guidelines of Columbia University Institutional Animal Care and Use Committee.

2.4. Focused ultrasound sonication with microbubbles

Mice were sonicated at the targeted brain location using an experimental setup that was illustrated in Tung et al. (Tung et al., 2011), following an experimental timeline shown in Fig. 1. Mouse heads were immobilized using stereotaxic frame (David Kopf Instruments, Tujunga, CA, USA). The fur on the head and tail was removed with an electrical trimmer and a depilatory cream, while the scalp and skull remained intact. A spherical, single-element FUS transducer (center frequency 1.5 MHz) and a pulse-echo transducer (center frequency 7.5 MHz), used for passive cavitation detection, confocally mounted at the center of the FUS transducer, were used. A custom-built cone was attached to the transducer and filled with degassed water to provide acoustic coupling and the cone was immersed in a degassed water container. The container was placed on the mouse head and coupled with ultrasound gel. The whole procedure was performed under anesthesia with 1–2% isoflurane in oxygen. Mice were placed on a heating pad with a constant temperature of approximately 40 °C to maintain the body temperature (Chen et al., 2014).

Before sonication, a grid system was used for targeting and the focal point of the FUS was located 3 mm beneath the skull, at approximately the center of the hippocampus, following the procedure that has been described elsewhere (Choi et al., 2007a, 2007b). The targeted region for each mouse was the left hemisphere. The right hemisphere of each animal served as its own control, reducing the variability caused by physiological differences among animals.

In this study, ultrasound exposure with a pulse length of 6.56 ms, pulse repetition frequency 5 Hz and a peak of acoustic pressure of 450 kPa was applied to the left hemisphere. The total sonication time was 2.5 min. Prior to microbubbles and rh BRICHOS administration, a 30 s sonication was applied using the acoustic parameters described above in order to measure the baseline background signal. 50 μ L of monodisperse lipid microbubbles were diluted in saline solution (8×10^8 microbubbles/mL) together with rh proSP-C BRICHOS or Bri2 BRICHOS-AU1 to achieve a dose of 1 or 10 mg/kg body weight, and administrated intravenously *via* the tail vein and immediately followed by 2 min of sonication.

2.5. MRI

After sonication, BBB opening was confirmed with T_1 -weighted

contrast enhanced magnetic resonance imaging (MRI) by a 9.4-T MRI system (Bruker Medical, Boston, MA). At 2 h after sonication, the mice were transcardially perfused with PBS for 5 min followed by perfusion with 4% paraformaldehyde (PFA) for 7 min. The brains were extracted from the skull and post-fixed in PFA for 48 h before being embedded in paraffin in order to perform histological analysis.

2.6. Antibodies used for immunohistochemistry (IHC), immunofluorescence (IF), western blots and ELISA

For IHC, primary antibodies, their antigens and dilutions were: polyclonal rabbit anti-surfactant protein-C (Atlas Cat# HPA010928, anti-SFTPC), 1:200; polyclonal rabbit anti-AU1 (Abcam Cat#ab3401), 1:200; monoclonal mouse anti-NeuN (Merck Cat#MAB377). For IF, primary antibodies were: polyclonal rabbit anti-surfactant protein-C (Atlas Cat# HPA010928, anti-SFTPC), 1:200; polyclonal rabbit anti-AU1 (Abcam Cat#ab3401), 1:200; monoclonal mouse anti-doublecortin (Santa Cruz Cat#sc-271390, anti-DCX), 1:100; monoclonal mouse anti-EEA1 (Sigma-Aldrich Cat#E7659), 1:800. Secondary antibodies for IF microscopy were: alkaline phosphatase (AP) conjugated goat anti-rabbit (Biocare Medical, Cat#MRCT525); biotinylated goat anti-mouse, 1:200 (Vector Laboratories Inc., Cat#BA-9200); Alexa Fluor 546 conjugated goat anti-rabbit (Thermo Fisher, Cat#A-11035), 1:500. For western blots, primary antibodies and dilutions used were: polyclonal rabbit anti-AU1 (Abcam Cat#ab3401), 1:600; goat anti-Bri2 BRICHOS, 1:250. Fluorescently labeled secondary anti-rabbit or anti-goat antibodies (Li-Cor, Cat#926-32213), 1:10,000. For sandwich ELISA, as capture antibody goat anti-Bri2 BRICHOS was used, 1:250, and as detection antibody polyclonal rabbit anti-AU1 (Abcam Cat#ab3401), 1:2000 was used. Secondary anti-rabbit antibody conjugated with horseradish peroxidase (HRP), was diluted 1:2000 (GE Healthcare Cat#NA934).

2.7. Histological and IHC analyses

Coronal sections at 5 μ m thickness were obtained from paraffin embedded tissue using a microtome. The sections were placed onto Superfrost Plus microscope glass slides (Thermo Scientific) and were let dry at room temperature (RT) overnight to remove residual water. Sections were de-paraffinized by washing in xylene and re-hydrated in decreasing concentrations of ethanol (from 99% to 70%). Sections were pressure boiled in a Decloaking Chamber (Biocare Medical) immersed in DIVA decloaker solution 1X (Biocare Medical, Concord, USA) at 110 °C for 30 min, or incubated in a water bath heated at 95 °C for 30 min. Slides were let cool down at RT for 20 min, then washed with PBS buffer containing 0.1% tween 20 (PBST) and incubated with peroxidase blocking solution (Dako) for 5 min. The sections were washed in Tris-buffered saline (TBS) and additional blocking was performed with Background punisher (Biocare) for 10 min. Primary antibodies diluted in DAKO (Agilent) antibody diluent were incubated for 45 min

Table 1

BRICHOS delivery by FUS + MB. Summary of the groups of mice that were treated with rh proSP-C BRICHOS or Bri2 BRICHOS-AU1, doses, results of the delivery 2 h after administration and the brain areas where the respective BRICHOS domains were detected. One control mouse was not treated with FUS + MB or administered BRICHOS.

Protein delivered	Dose (mg/kg)	Successful delivery	Brain areas with positive detection
ProSP-C BRICHOS	1	0 of 3	No delivery
ProSP-C BRICHOS	10	2 of 3	Ipsilateral hippocampus
ProSP-C BRICHOS	10	2 of 3	Ipsilateral cortex
Bri2 BRICHOS-AU1	10	5 of 6	Both hemispheres: cortex, hippocampus, ventricles
Bri2 BRICHOS-AU1	10	2 of 2	Both hemispheres: cortex, hippocampus, ventricles
Bri2 BRICHOS-AU1	10	2 of 2	Both hemispheres from western blot and ELISA analyses

at RT. Negative control slides were incubated with the Dako antibody diluent only. Slides were washed in TBS and incubated with Mach 2 Double stain 2 containing conjugated secondary anti-rabbit-AP and/or anti-mouse HRP (Biocare Medical) for 30 min at RT. AP staining was detected with permanent red (Biosite) and horseradish peroxidase staining was visualized with the permanent green (Biosite). Sections were counterstained with hematoxylin solution (Mayer) to visualize nuclei, de-hydrated through ethanol (from 70% to 99%), cleared in xylene and mounted with DEPEX mounting media (Merck).

The tissue integrity after FUS was evaluated after hematoxylin and eosin staining for microscopic damage or microhemorrhages. Delivery was evaluated by staining for rabbit anti-SFTPC or rabbit anti-AU1; colocalization with neurons was studied using mouse anti-NeuN antibody.

2.8. Immunofluorescence

For determination of intracellular localization of BRICHOS proteins, immunofluorescence and microscopy were used. To examine proSP-C BRICHOS, doublecortin (anti-DCX) and early endosomes (anti-EEA1) colocalization, deparaffinization and antigen retrieval were performed as described above under immunohistochemical analyses. TSA Plus Fluorescein Evaluation detection system (PerkinElmer, Lot#2466870) was used to detect early endosomes and doublecortin positive cells. Briefly, after blocking with TNB (0.1 M Tris-HCl, 0.15 M NaCl, 0.5% (w/v) blocking reagent, pH 7.5) buffer for 30 min, mouse anti-DCX or mouse anti-EEA1 primary antibodies diluted in TNB buffer were incubated over night at 4 °C. The following day, brain sections were washed in PBS and incubated with secondary antibody conjugated with biotin diluted in TNB buffer for 2 h. Then, excess secondary antibodies were washed away with PBS and sections incubated with 1:100 SA-HRP in TNB buffer for 30 min, followed by washes with PBS and incubation with fluorophore Tyramide diluted 1:50 in Amplification Reagent for 10 min. To investigate rh Bri2 BRICHOS-AU1 subcellular localization, slides were deparaffinized and antigen retrieval was performed as described above. Staining against AU1 was performed as described above under immunohistochemical analyses section, using the same Mach 2 Double stain 2 containing conjugated secondary anti-rabbit AP (Biocare Medical) procedure. After AP detection with permanent red (Biosite), sections were de-hydrated with ethanol, cleared in xylene and then, re-hydrated in decreasing concentrations of ethanol, rinsed in water and washed in PBS. The second primary antibody, against early endosomes, was incubated in TNB blocking buffer over night at 4 °C after sections were blocked with TNB blocking buffer. The day after, sections were washed in PBS and incubated for 2 h with secondary antibody conjugated with biotin at a 1:200 dilution in TNB buffer. Thereafter, sections were washed in PBS and incubated with SA-HRP diluted 1:100 in TNB buffer at RT for 30 min, followed by washes in PBS and 10 min incubation of fluorophore Tyramide diluted 1:50 in Amplification Reagent (TSA kit Perkin Elmer). Lastly, all sections were incubated with Hoechst solution for 15 min, washed in PBS and slides were mounted with PermaFluor water soluble mounting media.

2.9. Microscopy

Bright-field images of stained sections were acquired using a Nikon Eclipse E800M optical microscope with a Plan-Apochromate 10×, 20× and 40× objectives. Both sonicated and non-sonicated hippocampi were evaluated. Fluorescence imaging was performed with a confocal laser scanning system or IF microscope. The fluorescence was recorded sequentially in separate channels with 20× objective. Fluorescence imaging was obtained with a Nikon fluorescence microscope. Fiji software (version 2.0.0-rc-65/1.51v) (Schindelin et al., 2012) was used for image processing.

2.10. Western blotting

Brain tissue from two mice treated with FUS + MBs and rh Bri2 BRICHOS-AU1 and one mouse that was not given BRICHOS injection or FUS + MBs treatment (negative control) were homogenized in 50 mM Tris-HCl, pH 7.4, 150 mM NaCl, 1% (v/v) Triton X-100, 0.1% (w/v) SDS and 10 mM EDTA supplemented with protease inhibitor cocktail (Roche, Indianapolis, IN). Homogenates were centrifuged at 14,000 rpm for 30 min at 4 °C, and the supernatant was collected and stored at −20 °C. Protein concentration was measured by BCA method. The brain homogenates were normalized to 100 µg total protein per sample by adding homogenization buffer and 1× SDS reducing buffer (containing 2-mercaptoethanol). The samples were heated at 97 °C for 10 min and separated on 4–20% precast polyacrylamide gel (Bio-Rad) and blotted on a nitrocellulose (GE Healthcare) membrane. After blotting, the membranes were blocked using 5% skim milk prepared in 0.1% Tween/TBS for 1 h at RT. Thereafter they were rinsed with 0.1% Tween/TBS and primary antibody diluted in 0.1% Tween/TBS was added over night at 4 °C. The membranes were washed three times with 0.1% Tween/TBS and then incubated with secondary antibody prepared in 0.1% Tween/TBS for 1 h at RT. After washing the unbound secondary antibody with 0.1% Tween/TBS, the image was acquired using a fluorescence imaging system (Li-Cor, Odyssey CLx).

2.11. Sandwich ELISA

96-well plates (Nunc MicroWell™) were coated with capture antibody (anti Bri2 BRICHOS) diluted in coating buffer (50 mM carbonate pH 9.6) and incubated overnight at 4 °C. After washing three times with 0.05% Tween/PBS, 1% BSA/PBS was used for blocking for 1 h. Following the washing and blocking steps, the brain samples (250 µg/mL, 100 µL) and standards diluted in 0.05% Tween/PBS were incubated for 2 h at RT. The plate was washed and a primary antibody (rabbit anti-AU1) diluted in 0.05% Tween/PBS was added over night at 4 °C. The plate was washed three times and a secondary anti-rabbit antibody diluted in 0.05% Tween/PBS was added for 2 h at RT. After washing the plate, tetramethylbenzidine (TMB) (Thermo Fisher) solution was added and incubated for 30 min in darkness. The reaction was stopped by adding stop solution for TMB substrates (Thermo Fisher) and absorbance was measured at 450 nm, using the values for brain homogenates from the non treated mouse as blank. The standard curve was obtained

proSP-C BRICHOS injected, proSP-C BRICHOS stained

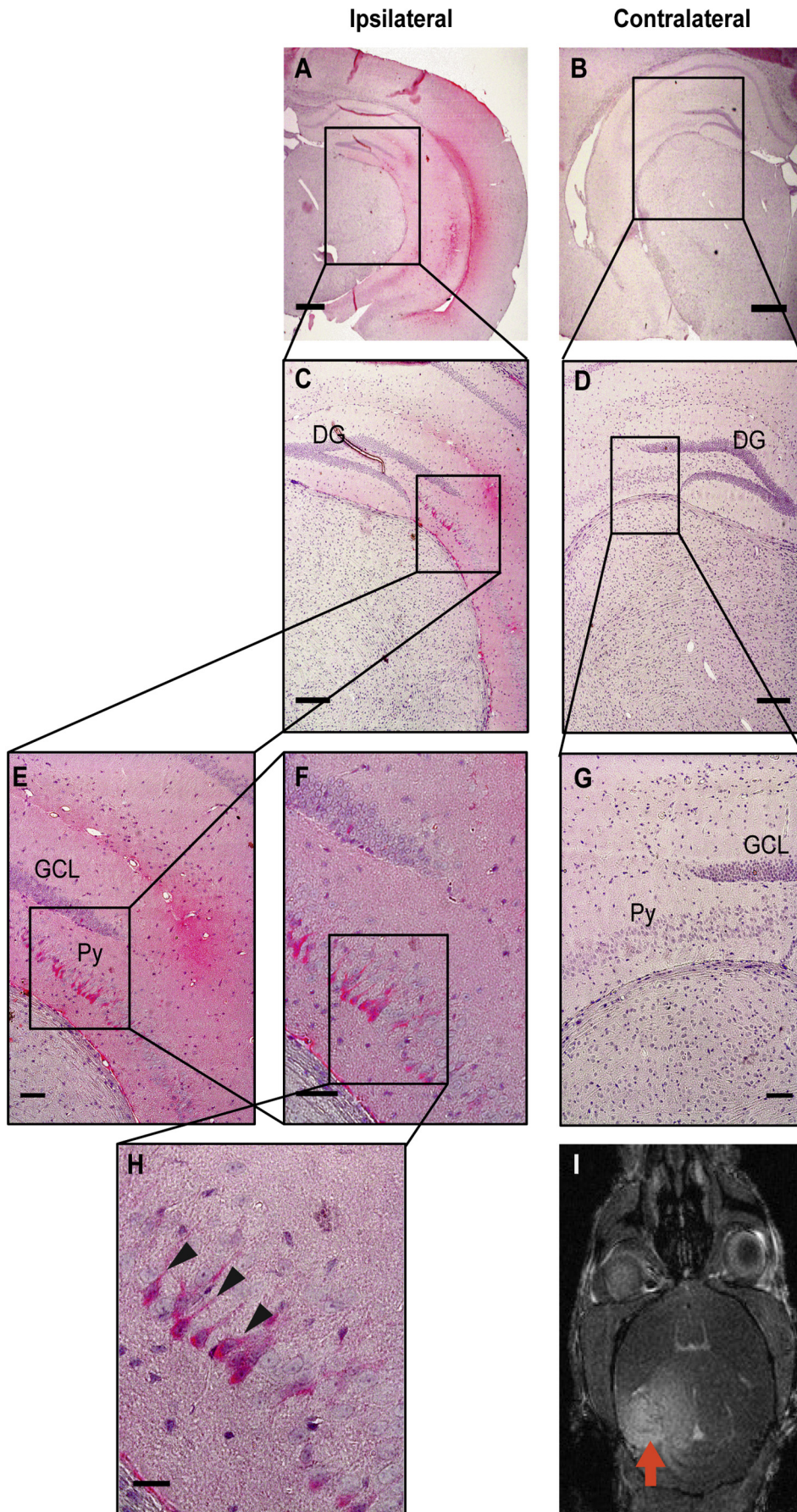


Fig. 2. Rh proSP-C BRICHOS is detected in the FUS + MB-targeted hippocampal region. (A-H) Immunohistochemistry for rh proSP-C BRICHOS in FUS + MB-targeted ipsilateral hippocampal sections compared to the contralateral, non-targeted side. Sections were immunostained with anti-proSP-C antibody followed by an alkaline phosphatase (AP) conjugated secondary antibody and developed with permanent red AP solution. All samples are counterstained with hematoxylin. The arrowheads in (H) indicate some of the cells that show intracellular staining for proSP-C BRICHOS. (I) Successful opening of the BBB in the ipsilateral side is demonstrated with contrast-enhanced T1-weighted MRI. The targeted region in the hippocampus is indicated with a red arrow. DG, dentate gyrus; GCL, granule cell layer; Py, pyramidal cell layer. Sizes of scale bars are: 200 μ m (A, B), 100 μ m (C, D), and 50 μ m (E-H). (For interpretation of the references to colour in this figure legend, the reader is referred to the web version of this article.)

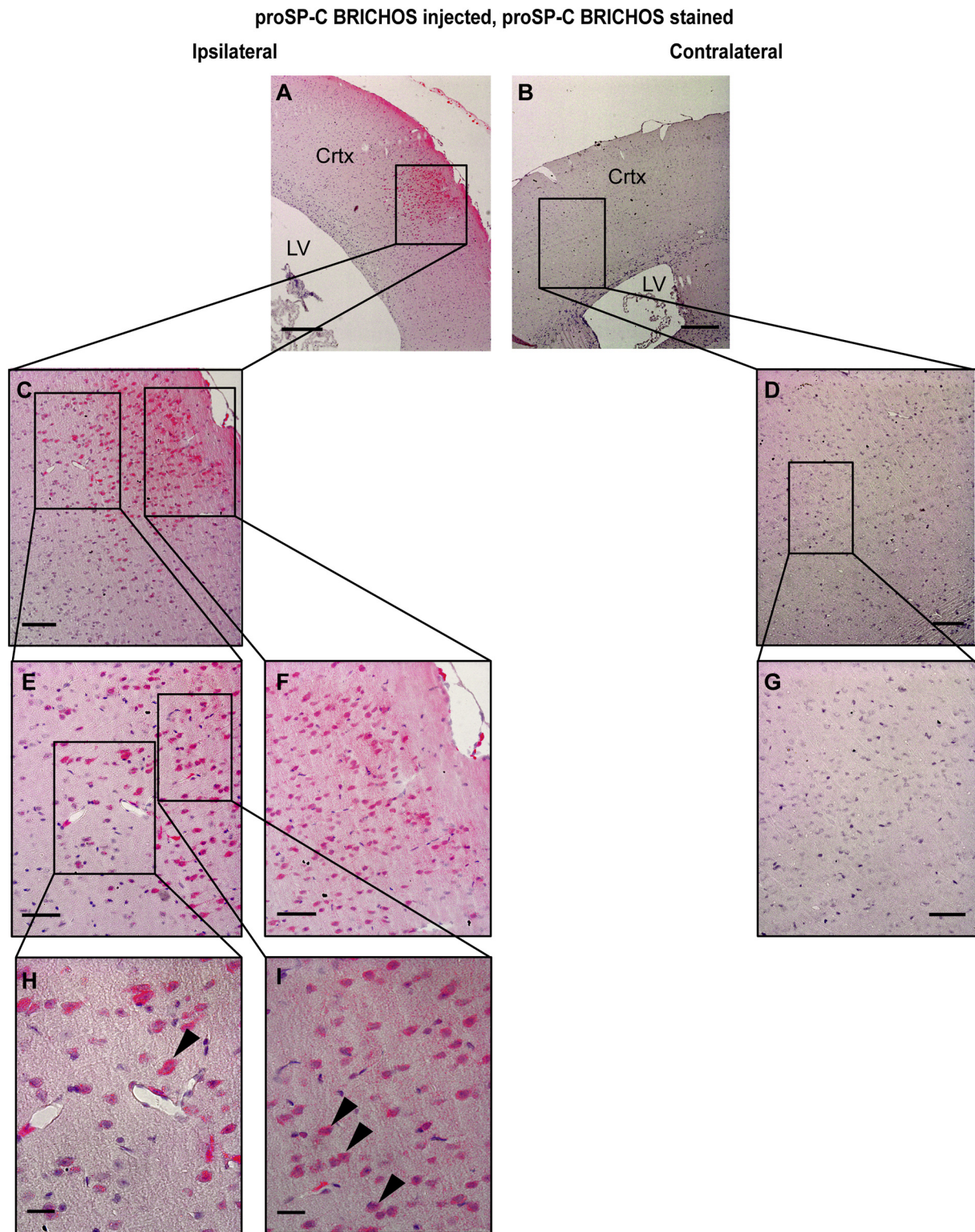


Fig. 3. Detection of rh proSP-C BRICHOS in the cortex after FUS + MB. (A-I) rh proSP-C BRICHOS is found in FUS-targeted cerebral cortex but not in the contralateral side. Tissues are stained with a rabbit anti-proSP-C antibody followed by AP conjugated secondary antibody and developed with permanent red AP solution. Samples were counterstained with hematoxylin. The intracellular proSP-C BRICHOS staining is indicated by arrowheads. Boxed areas are zoomed in and scale bars are indicated. LV, lateral ventricle; Crtx, cortex. Scale bars are: 500 μ m (A, B), 200 μ m (C, D), 100 μ m (E-G) and 50 μ m (H, I).

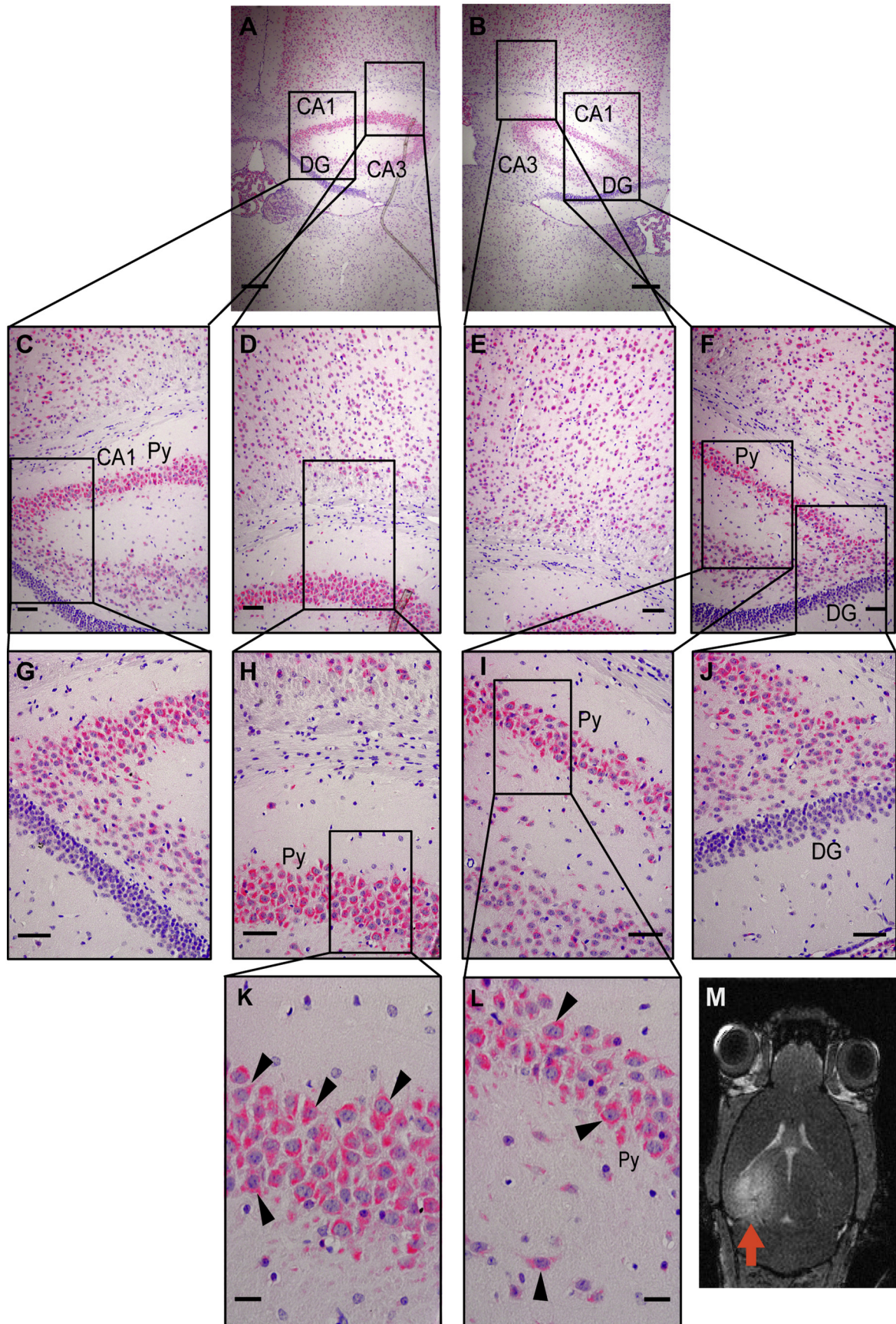
from rh Bri2 BRICHOS-AU1 protein ranging from 0.1 to 64 ng. Calculation of total amount of rh Bri2 BRICHOS-AU1 in each brain hemisphere was assessed by assuming a brain density of 1.04 mg/mL, an average brain hemisphere weight of 225 mg and average of total protein in brain hemisphere homogenate of 25.6 mg.

3. Results

3.1. Overall study design

Rh proSP-C BRICHOS or rh Bri2 BRICHOS-AU1 were administered

Bri2 BRICHOS-AU1 injected, Bri2 BRICHOS-AU1 stained
Ipsilateral **Contralateral**



(caption on next page)

Fig. 4. Rh Bri2 BRICHOS-AU1 is found in ipsilateral and contralateral hemispheres after FUS + MB. (A-L) Immunohistochemistry for rh Bri2 BRICHOS-AU1 in sections from FUS + MB-targeted ipsilateral and contralateral, non-targeted hippocampus. Sections were immunostained for rh Bri2 BRICHOS-AU1 using an anti-AU1 tag antibody followed by AP conjugated secondary antibody and developed with permanent red AP solution. The tissues were counterstained with hematoxylin. The arrowheads in K and L indicate cells that show intracellular staining for Bri2 BRICHOS-AU1. (M) Although rh Bri2 BRICHOS-AU1 is observed in both hemispheres, BBB opening occurs only in the ipsilateral side as observed by contrast-enhanced T1-weighted MRI, red arrow indicates targeted area. Images are representative of 4 independent experiments. CA1-CA3 fields are labeled. DG, dentate gyrus; Py, pyramidal cell layer. Sizes of scale bars are: 200 μ m (A, B), 100 μ m (C-F), 50 μ m (G-J) and 20 μ m (K, L). (For interpretation of the references to colour in this figure legend, the reader is referred to the web version of this article.)

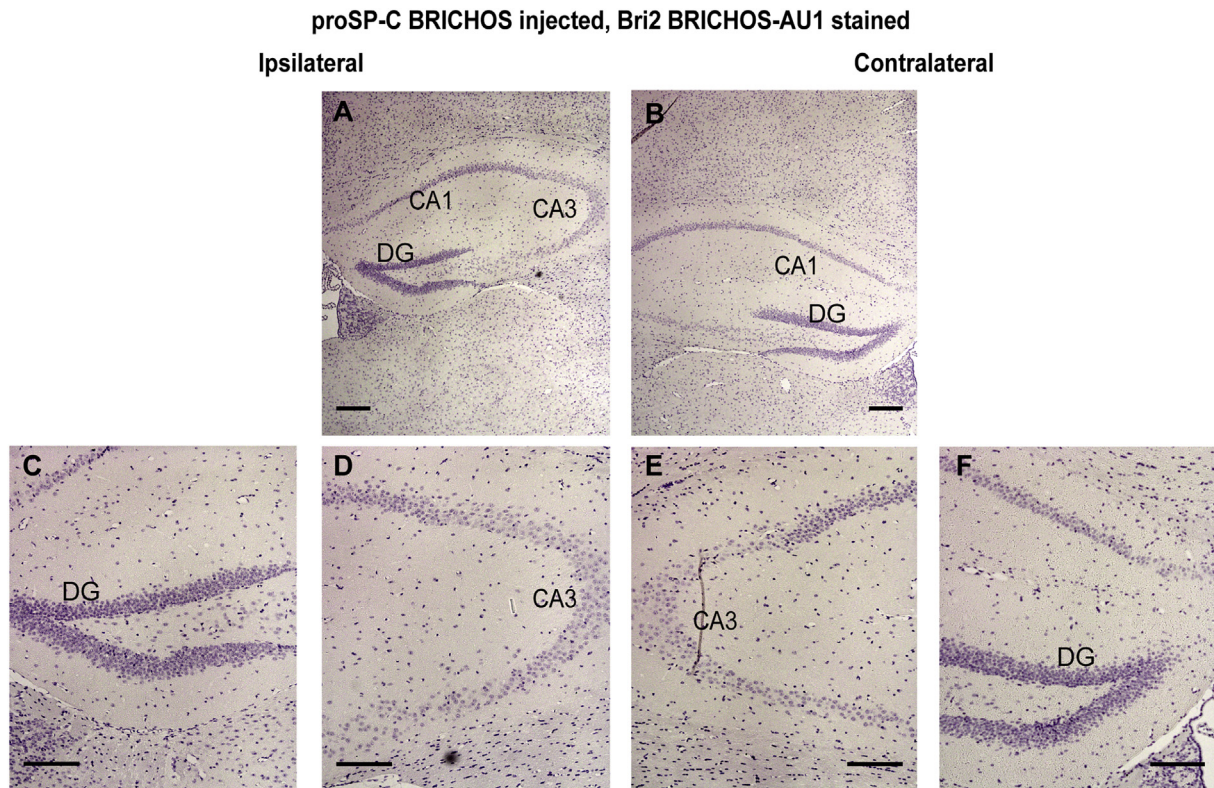


Fig. 5. No staining with anti-AU1 antibody in proSP-C BRICHOS delivered mice. No anti-AU1 antibody staining is found in the hippocampus area from FUS + MB-treated mice injected with 10 mg/kg of rh proSP-C BRICHOS. (A-F) sections were stained with rabbit anti-AU1 tag primary antibody followed by AP conjugated secondary antibody and developed with permanent red AP solution. All samples were counterstained with hematoxylin. CA1-CA3 field; DG, dentate gyrus. Sizes of scale bars are 200 μ m. (For interpretation of the references to colour in this figure legend, the reader is referred to the web version of this article.)

at doses of 1 and 10 mg/kg body weight together with MBs via the tail vein. Immediately before and after injection, FUS was targeted to the left hippocampus for 30 s and 2 min, respectively (Fig. 1). Animals underwent MRI after the second sonication to verify BBB opening, and were sacrificed 2 h after FUS + MB administration (Fig. 1). In contrast to proSP-C BRICHOS, whose expression is restricted to alveolar type II cells (Glasser et al., 1990), Bri2 is expressed in the CNS (Lashley et al., 2008; Zeisel et al., 2015). This requires that exogenously delivered rh Bri2 BRICHOS can be distinguished from endogenous Bri2. We therefore used a version of rh Bri2 BRICHOS that carries an AU1 tag for immunodetection (Tambaro et al., 2019). Rh Bri2 BRICHOS-AU1 behaves like rh Bri2 BRICHOS as regards expression and purification (Supplementary Fig. S1), inhibition of A β 42 fibril formation, and can be distinguished from endogenous Bri2 in mouse brain homogenates (Tambaro et al., 2019).

A total number of 20 mice were used in this study. Initially three mice were administered 1 mg/kg of rh proSP-C BRICHOS, but immunohistochemistry (IHC) failed to detect any protein delivered to the brain, and, hence, subsequently doses of 10 mg/kg of rh proSP-C or Bri2 BRICHOS were used (Table 1). One mouse treated with 10 mg/kg rh proSP-C BRICHOS died immediately after sonication and no positive staining for rh proSP-C BRICHOS was detected. In one group of three mice administered with rh proSP-C BRICHOS, the left cortex was inadvertently targeted by FUS, and delivery into the cortex was then

observed in 2 of these mice. In one group of mice treated with rh Bri2 BRICHOS-AU1, one mouse died 15 min after sonication, however protein delivery was observed also in this case. Lastly, three mice were used to further evaluate rh Bri2 BRICHOS-AU1 delivery by western blot and ELISA analyses.

Since microbubble oscillations may exert excessive stress on the vascular walls, thereby compromising safety, tissue integrity was assessed by histological analyses after hematoxylin-eosin staining.

We found that areas corresponding to sonicated regions appeared histologically normal in both rh proSP-C and Bri2 BRICHOS administered mice (Supplementary Fig. S2, panels A-J). One rh Bri2 BRICHOS-AU1 FUS + MB treated mouse showed clusters of extravasated erythrocytes in the sonicated region but no tissue damage was detected in the contralateral side (Supplementary Fig. S2, panels K-N). Thus, in 13 out of 16 cases treated with 10 mg/kg BRICHOS, BBB opening was achieved and delivery of rh BRICHOS domains was successful.

3.2. Rh proSP-C BRICHOS is delivered to the brain parenchyma by FUS + MB

FUS + MB significantly enhanced delivery of rh proSP-C BRICHOS in the targeted left hippocampus compared with the contralateral right side as judged by IHC (Fig. 2). Rh proSP-C BRICHOS is internalized by pyramidal cells in the CA3 region in the hippocampus (Fig. 2, panel H,

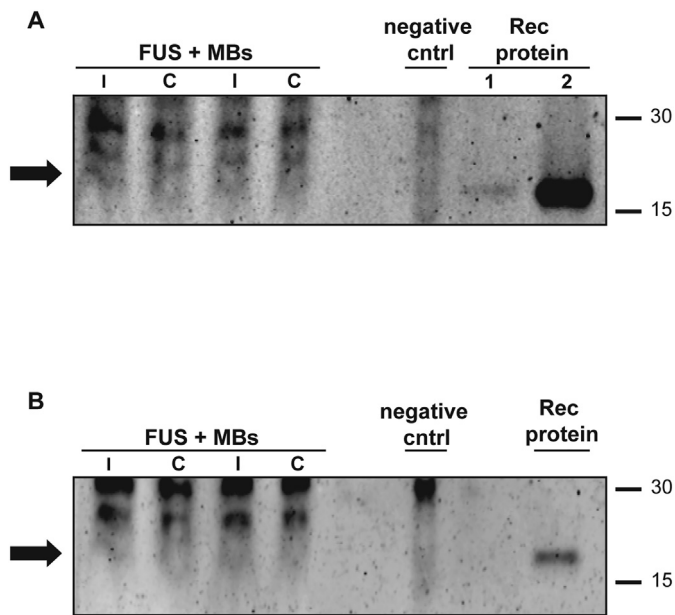


Fig. 6. Rh Bri2 BRICHOS-AU1 is detected in both hemispheres after intravenous injection together with FUS + MBs. Western blot analysis of brain hemispheres (I, ipsilateral side; C, contralateral side) homogenates from two mice collected 2 h after treatment with rh Bri2 BRICHOS-AU1 and FUS + MBs, and brain hemisphere from a non-sonicated, non-treated control mouse (negative control). Rh Bri2 BRICHOS-AU1 is detected using an anti-AU1 tag antibody in panel A, and using an anti-Bri2 BRICHOS antibody in panel B. Lanes marked Rec protein contain different amounts of rh Bri2 BRICHOS.

arrowheads). Furthermore, in two mice in which the left cortex was inadvertently targeted by FUS + MB, rh proSP-C BRICHOS was efficiently delivered and got internalized by cells in the cortex, while the contralateral, non-targeted hemisphere, showed no positive staining (Fig. 3). Specificity of the antibody against rh proSP-C BRICHOS was verified in brain tissue from a FUS + MB-treated mouse that had been administered with 10 mg/kg of rh Bri2 BRICHOS-AU1, showing no immunohistochemical staining (Supplementary Fig. S3).

3.3. Rh Bri2 BRICHOS-AU1 is delivered to both hemispheres after targeted FUS + MB

Rh Bri2 BRICHOS-AU1 was detected to the same extent in both the FUS-targeted hemisphere and in the contralateral hemisphere, by IHC using antibodies against the AU1 tag (Fig. 4). Although IHC intensity and distribution observed for rh Bri2 BRICHOS-AU1 in the targeted and non-targeted area are similar, the BBB opening occurred only in the ipsilateral side, as confirmed by MRI (Fig. 4, panel M). Furthermore, intracellular immunoreactivity was observed both in cells in the cortex and in the hippocampus (Fig. 4, panels K, L). The distribution pattern of rh Bri2 BRICHOS-AU1 and rh proSP-C BRICHOS in the hippocampus are different (Figs. 2 and 4). Control experiments in which brain sections from mice that had been FUS + MB treated and injected with rh proSP-C BRICHOS were stained for rh Bri2 BRICHOS-AU1 showed no immunoreactivity (Fig. 5).

3.4. Similar levels of delivered rh Bri2 BRICHOS-AU1 in both brain hemispheres

10 mg/kg of rh Bri2 BRICHOS-AU1 was administered to two mice followed by FUS + MBs, and brain penetration of the recombinant protein was evaluated after 2 h. Western blot analysis of brain hemisphere homogenates using anti-AU1 or anti Bri2 BRICHOS antibodies showed a band migrating like rh Bri2 BRICHOS-AU1, which was not detected in a negative control sample (Fig. 6). In order to provide a

quantitative measure of the amount of rh Bri2 BRICHOS-AU1 that passes the BBB, sandwich ELISA was performed from the individual hemisphere homogenates. ELISA analysis revealed that the rh Bri2 BRICHOS-AU1 concentration in the left hemisphere was about 120 nM while in the right hemisphere it was 150 nM. This supports the observation from immunohistochemistry (Fig. 4) that the amount of rh Bri2 BRICHOS is very similar in the two hemispheres. The rh Bri2 BRICHOS-AU1 detected in the brain homogenates by ELISA corresponded to 0.4% of the total amount administered.

3.5. Rh BRICHOS proteins are taken up by neuronal cells

To determine the identity of the cells in the hippocampus that take up rh proSP-C and rh Bri2 BRICHOS-AU1 (Figs. 2 and 4), we double-stained the brain sections for NeuN, a marker for mature neurons, and proSP-C BRICHOS (Fig. 7, panels A–J) or rh Bri2 BRICHOS-AU1 (Fig. 8), respectively. The BRICHOS proteins were taken up by neuronal cells; rh proSP-C BRICHOS is observed in a subset of cells in the granular cell layer of dentate gyrus in the hippocampus (Fig. 7), while rh Bri2 BRICHOS-AU1 is taken up mainly by pyramidal cells in the CA1 and CA3 hippocampal region (Fig. 8). Due to the observed specificity of BRICHOS uptake, especially for rh proSP-C BRICHOS in the subgranular zone of dentate gyrus of the sonicated hippocampus (Fig. 7, panels A–J), we also investigated whether rh proSP-C BRICHOS co-localizes with doublecortin (DCX), a marker for immature neurons. However, DCX positive cells do not stain for rh proSP-C BRICHOS (Fig. 7, panels K–Q).

3.6. Rh proSP-C and Bri2 BRICHOS intracellular localization

Next, we investigated whether the rh BRICHOS proteins were localized to early endosomes using fluorescence microscopy for proSP-C BRICHOS, Bri2 BRICHOS-AU1 and early endosomes using EEA1 as marker. Fig. 9 and Supplementary Fig. S4 show rh proSP-C BRICHOS localization mainly in the granular cell layer of the dentate gyrus, and images with merged rh proSP-C BRICHOS and EEA1 staining reveal that most of the intracellular proSP-C BRICHOS does not colocalize with early endosomes. Likewise, most of the intracellular rh Bri2 BRICHOS-AU1 in the ipsilateral pyramidal cell region is not found in early endosomes, although some areas where rh Bri2 BRICHOS-AU1 is localized in endosomes can be found (Fig. 10A and Supplementary Fig. S5). Similar results were obtained for the contralateral, non-targeted, hippocampus (Fig. 10B). As a control, a FUS + MB treated mouse that was administered with rh proSP-C BRICHOS was stained with the anti-AU1 antibody using the immunofluorescence protocol, and no positive staining was observed (Supplementary Fig. S6), again supporting that rh Bri2 BRICHOS-AU1 is delivered to both hemispheres after locally targeted BBB opening.

4. Discussion

The major findings of this study are that (i) rh proSP-C and Bri2 BRICHOS delivery to the brain parenchyma is feasible by FUS + MB; (ii) the two different rh BRICHOS proteins are taken up by distinct subsets of neurons in the hippocampus; (iii) rh Bri2 BRICHOS targeted to one hemisphere is found also in the contralateral non-targeted hemisphere; (iv) both rh proSP-C and Bri2 BRICHOS colocalize only to a minor extent with early endosomes in hippocampal neurons; and (v) FUS does not cause parenchymal damage or microhemorrhages in most cases.

The present study supports that FUS + MB technology is a safe way to deliver proteins over the BBB in mice. In this study, we focused on the hippocampus, as this region is central to the pathology in AD (Halliday, 2017). Our results show rh proSP-C and Bri2 BRICHOS delivery in the ipsilateral area of mouse hippocampus in 13 out of 16 mice that received a dose of 10 mg/kg. We first applied 1 mg/kg dose of rh BRICHOS domain, but delivery was not observed, therefore 10 mg/kg

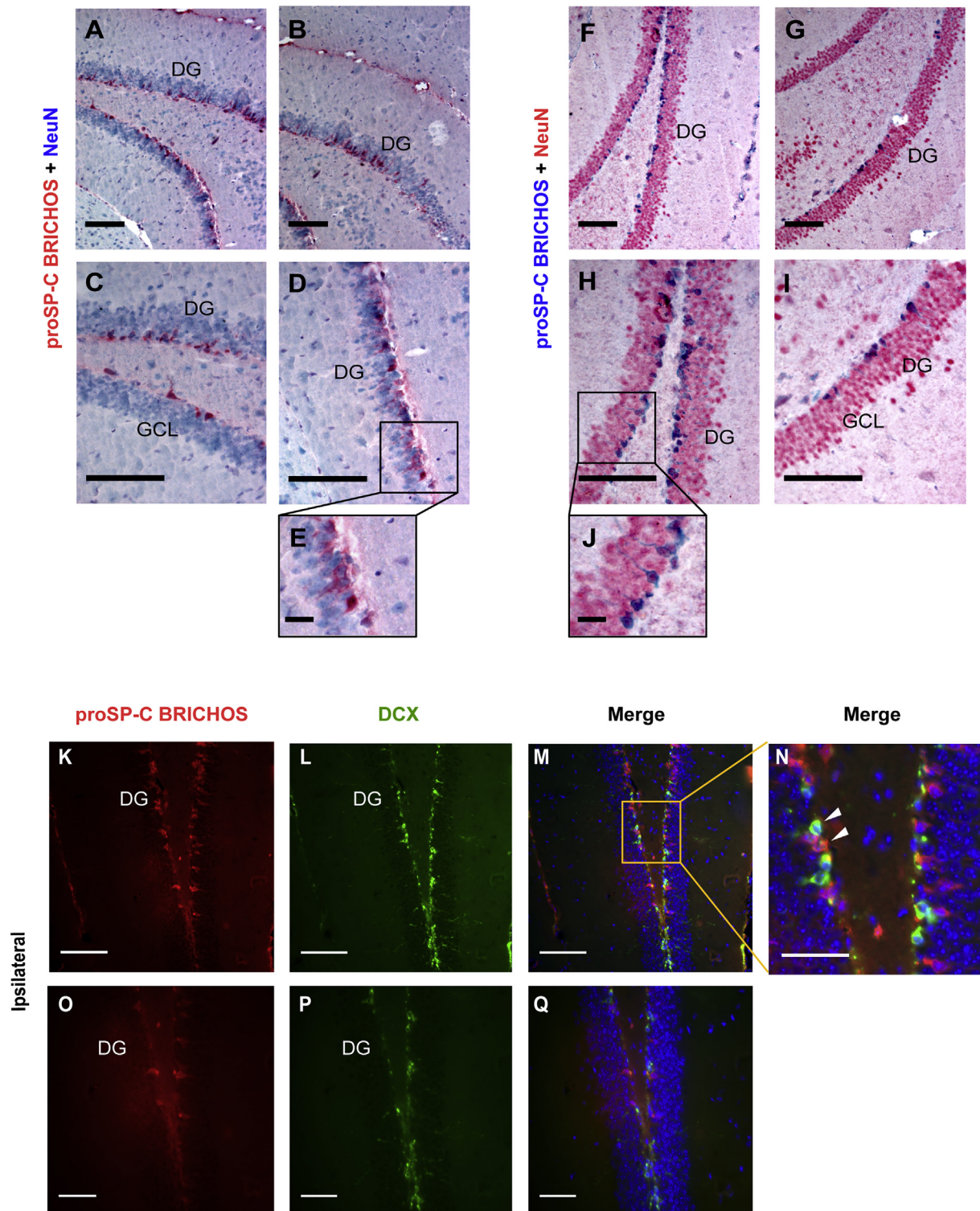


Fig. 7. Rh proSP-C BRICHOS in neurons after FUS + MB. Representative IHC double staining of rh proSP-C BRICHOS (red in panels A-E, blue in panels F-J) and mature neurons (anti-NeuN, blue in panels A-E, red in panels F-J) in the FUS + MB-targeted ipsilateral hippocampus. Tissues were stained with rabbit anti-proSP-C antibody and mouse anti-NeuN antibody followed by anti-rabbit AP and anti-mouse horse radish peroxidase (HRP) conjugated secondary antibodies and developed with permanent red AP solution or HRP green chromogen, respectively. Samples A-J were counterstained with hematoxylin. (K-Q) immunostaining of proSP-C BRICHOS (red) and immature granule cells using anti-doublecortin (anti-DCX antibody, green) marker in the dentate gyrus. Arrowheads in panel N indicate lack of co-localization of proSP-C BRICHOS with DCX. Nuclei were stained with Hoechst (blue). Boxes highlight zoomed in areas. Scale bar: 50 µm for all images. Abbreviations: DG, dentate gyrus; GCL, granular cell layer. Scales bars: 100 µm (A-D, and F-I), 50 µm (K-M and O-Q), 20 µm (E, J and N). (For interpretation of the references to colour in this figure legend, the reader is referred to the web version of this article.)

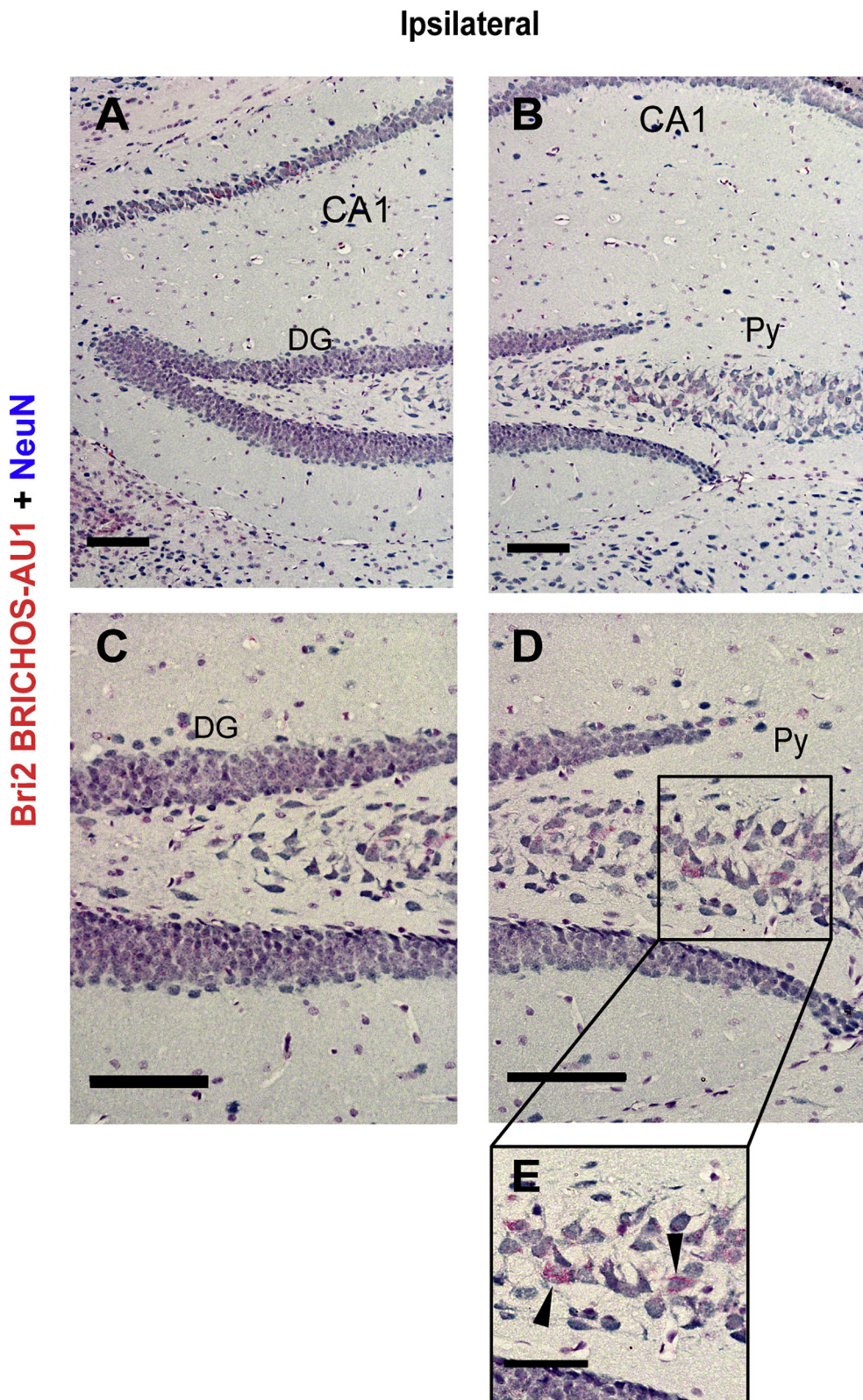


Fig. 8. Rh Bri2 BRICHOS-AU1 in neurons after FUS + MB. IHC double staining of FUS + MB-targeted hippocampus with anti-AU1 antibody (red) for detection of rh Bri2 BRICHOS-AU1 and anti-NeuN antibody (blue) for detection of mature neurons, followed by anti-rabbit AP and anti-mouse HRP conjugated secondary antibodies and development with permanent red AP and HRP solutions. All samples were counterstained with hematoxylin. Arrowheads in panel E highlight internalization of rh Bri2 BRICHOS-AU1 by neurons. Abbreviations: CA1, field CA1; DG, dentate gyrus, GCL, granular cell layer. Scale bars: 100 μm for images A-D, and 50 μm for pannel E. (For interpretation of the references to colour in this figure legend, the reader is referred to the web version of this article.)

was used in the following studies.

Interestingly, rh Bri2 BRICHOS protein was also found in the contralateral, non-targeted hemisphere by FUS + MB, although MRI confirmed that BBB opening was confined to the focused brain region. Furthermore, the rh Bri2 BRICHOS-AU1 concentrations determined by sandwich ELISA are similar in the ipsilateral and contralateral sides,

which is in agreement with the observation that rh Bri2 BRICHOS has the ability to cross the BBB without application of FUS + MB (Tambaro et al., 2019). Presence of erythrocyte extravasations was found in one mouse out of 14 administered with a dose of 10 mg/kg. It has been shown that chronic FUS treatment (up to 6 months) in mice does not cause any motor, behavioral or morphological alterations (Olumolade

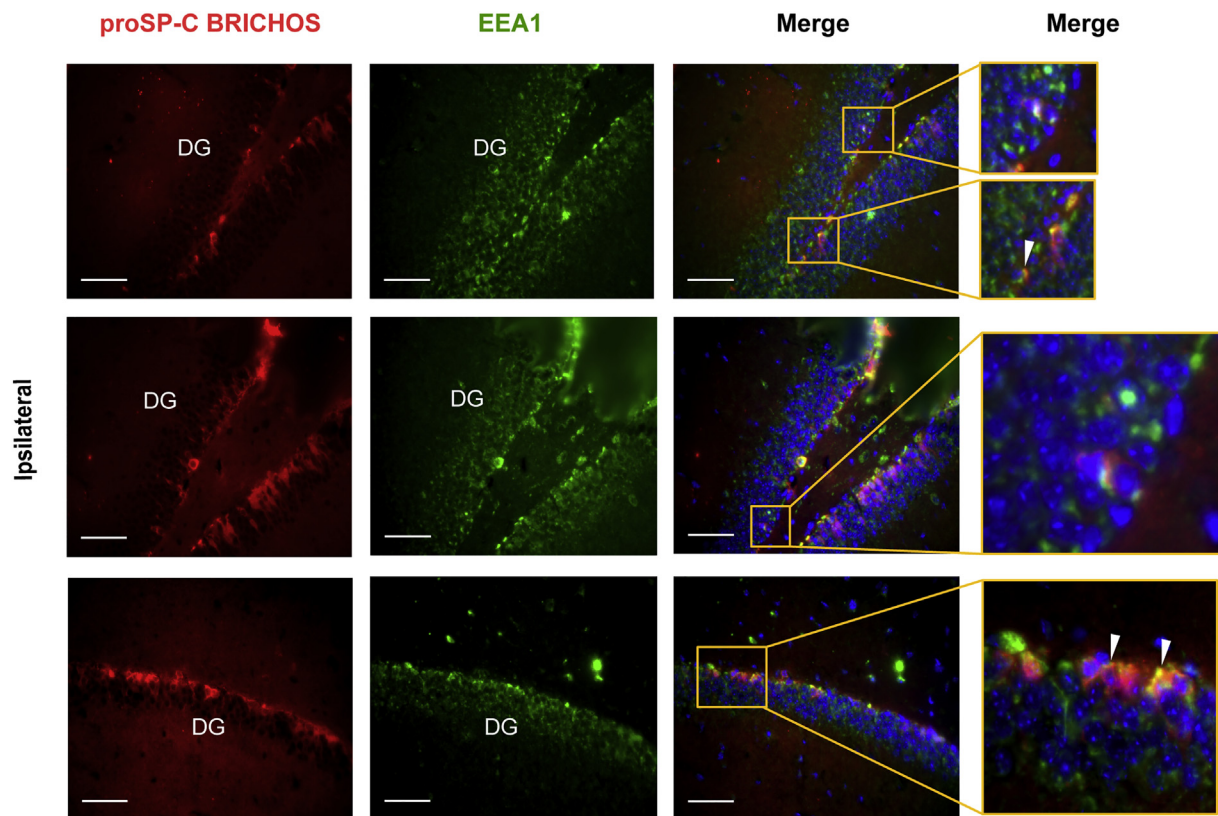


Fig. 9. Rh proSP-C BRICHOS and early endosome staining in neurons. Rh proSP-C BRICHOS (red) and early endosomes (green) in the granular cell layer of the FUS + MB-targeted hippocampus. Arrowheads in zoomed in areas in merged pictures indicate cases of co-localization of rh proSP-C BRICHOS and endosomes. Individual zoomed-in areas are shown in Supplementary Fig. S4. Nuclei were stained with Hoechst (blue). Abbreviations: DG, dentate gyrus. Scale bars: 50 μ m. (For interpretation of the references to colour in this figure legend, the reader is referred to the web version of this article.)

et al., 2016). Previous behavioral studies in non-human primates after consecutive FUS + MB treatments did not show abnormalities in behavior and normal appearing brain tissue even when small erythrocyte extravasations were present (McDannold et al., 2012). FUS + MB as a therapeutic method has been used in AD patients in a phase I safety trial, causing no adverse effects and supporting it as a potential strategy to treat brain diseases (Lipsman et al., 2018).

Rh proSP-C and Bri2 BRICHOS delivered by FUS + MB are internalized in distinct hippocampal locations (Figs. 7 and 8), which implies that neurons show selectivity in the uptake of different BRICHOS domains. Rh proSP-C BRICHOS is observed mostly in the granular cell layer of the sonicated hippocampus, although it was also detected intracellularly in some pyramidal cells in the CA3 region, while rh Bri2 BRICHOS-AU1 was detected in the hippocampal pyramidal cell layer in both hemispheres. Further analyses are required in order to determine the detailed distribution of administered BRICHOS domains. The mechanism whereby rh Bri2 BRICHOS-AU1 reaches the contralateral hemisphere as well as the reason why specific subsets of neurons take up BRICHOS remain to be established. Our previous study of spontaneous transfer of rh BRICHOS over the BBB found positive staining of rh Bri2 BRICHOS in the entire brain parenchyma, including the choroid plexus, after systemic administration. Additionally, in some cases positive rh Bri2 BRICHOS staining was detected intracellularly in the perinuclear area of cells in the cortex and striatum (Tambaro et al., 2019). A delivered fluorophore was found to transfer through the corpus callosum to the non-targeted hemisphere (Sierra et al., 2017) and downstream effects of FUS + MB delivered neurotrophic factors were observed in both the ipsilateral and contralateral sides (Baseri et al., 2012). However, in these cases the response in the contralateral side was small compared to the ipsilateral side, while in the case of rh Bri2 BRICHOS the responses by IHC, western blots (Figs. 4 and 6) and ELISA

are practically identical in both hemispheres. It has been shown that BBB permeability varies in different regions, for example in the lateral periventricular areas close to the choroid plexus, the BBB is not as impermeable as in the cortex (Strazielle and Gherzi-Egea, 2016; Ueno et al., 2000). Studies have reported an enhancement of doxorubicin uptake in endothelial cells when applying FUS + MBs (Arvanitis et al., 2018). Delivery of an anti-tau single chain antibody in a tau mouse model by scanning ultrasound was increased, not only in the brain parenchyma as a whole but also specifically in the cell body and dendrites of neurons (Nisbet et al., 2017). The two BRICHOS domains differ in many aspects; they show < 25% sequence identity, have different quaternary structures, are produced in different organs, and only rh Bri2 BRICHOS spontaneously passes the BBB (Tambaro et al., 2019). The gene coding for Bri2 (*ITM2B*) is highly expressed in pyramidal neurons in the CA1 region of the mouse hippocampus as observed using single cell RNA-sequencing (Zeisel et al., 2015). Interestingly, in humans *ITM2B* expression occurs in neurons in the hippocampus, especially pyramidal neurons in CA3 and CA4 regions, and in cells in the choroid plexus (Akiyama et al., 2004; Baron and Pytel, 2017), i.e. a similar pattern as the now observed cellular uptake.

Extracellular molecules that are taken up by endocytosis initially ends up in endosomes whereafter they can be routed to different cellular locations or be transcytosed (Villasenor et al., 2019). In most hippocampal regions there is no colocalization of rh BRICHOS proteins with early endosomes as judged by lack of general overlap after co-staining with the early endosome marker EEA1. These findings indicate that most of the FUS + MB-delivered rh BRICHOS proteins permeate into the cells without being carried by endosomes and/or escape the endosomal pathway efficiently.

Further research is warranted about physiological mechanisms of BRICHOS in relation to A β toxicity and plaque formation in the brain

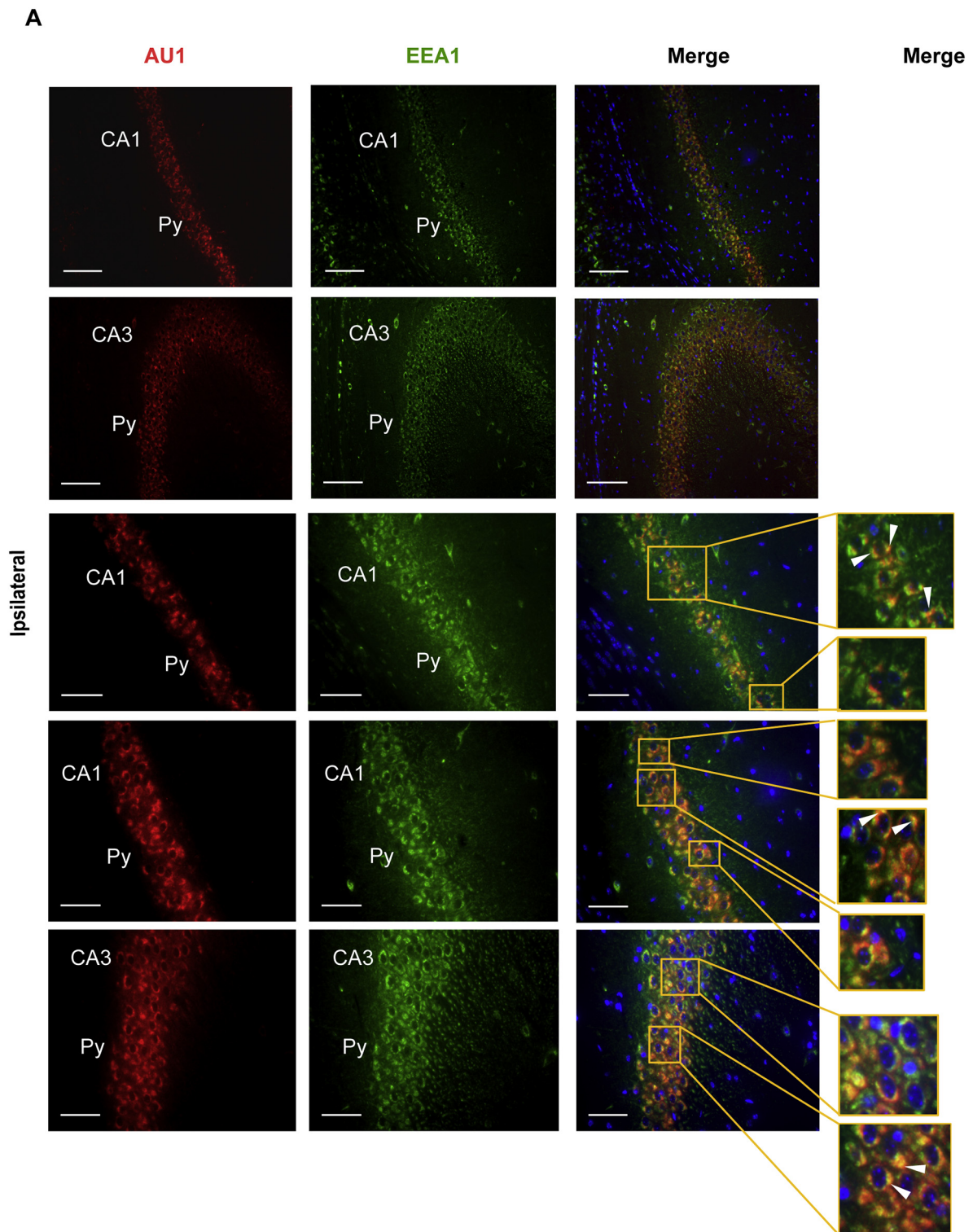


Fig. 10. Immunofluorescence of rh Bri2 BRICHOS-AU1 and early endosomes in neurons. Rh Bri2 BRICHOS-AU1 (red) and early endosomes (green) in pyramidal cells in the ipsilateral (A) and contralateral (B) hippocampus. Arrowheads point out cases of apparent co-localization of rh Bri2 BRICHOS-AU1 and early endosomes. Individual magnified regions are shown in Supplementary Fig. S5. Nuclei were stained with Hoechst (blue). Abbreviations: CA1-CA3, fields CA1 to CA3; Py, pyramidal cell layer hippocampus. Scale bars: 50 μ m. (For interpretation of the references to colour in this figure legend, the reader is referred to the web version of this article.)

using transgenic and knock-in mouse models for AD. In particular the ability of rh Bri2 BRICHOS to spontaneously pass the BBB (Tambaro et al., 2019), to be efficiently taken up in both hemispheres after FUS + MB and to be taken up by hippocampal neurons suggests that it can be useful in future treatment of AD.

Ethical approval

All animal procedures were done in accordance with the ethical standards of the National Institutes of Health (NIH) and Columbia University Institutional Animal Care and Use Committee gave approval

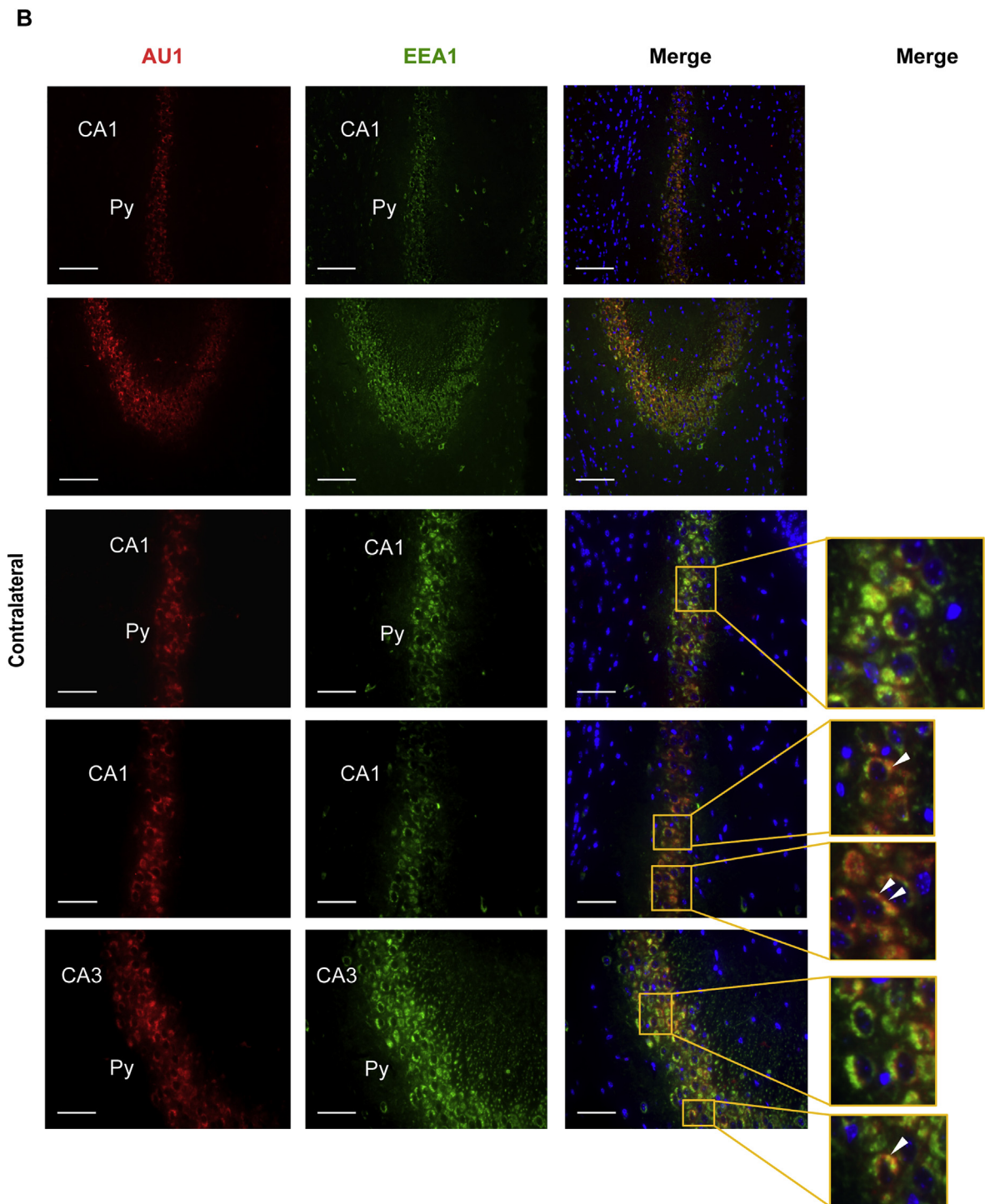


Fig. 10. (continued)

for the mouse studies. Approved licences: AC-AAAI1103 (Y3 M01) and AC-AAAS5550 (Y1 M00).

Funding

This work was supported by the Swedish Research Council (2016-01967), CIMED and VINNOVA (2016-04059).

Author statement

The BRICHOS domain is found in human precursor proteins

associated with cancer, dementia and amyloid lung disease and recombinant human BRICHOS domains delay amyloid- β peptide ($A\beta$) fibril formation and reduce associated toxicity *in vitro* and in animal models of Alzheimer's disease. Here we find that recombinant BRICHOS can be delivered to the brain parenchyma using targeted ultrasound and microbubbles. The BRICHOS domain derived from Bri2 was detected also in the non-targeted hemisphere and taken up by a subset of neurons in the hippocampus and cortex, indicating that rh Bri2 BRICHOS can be efficiently delivered into the mouse brain parenchyma.

Declaration of competing interest

Authors declare no conflict of interest.

Appendix A. Supplementary data

Supplementary data to this article can be found online at <https://doi.org/10.1016/j.mcn.2020.103498>.

References

- Akiyama, H., Kondo, H., Arai, T., Ikeda, K., Kato, M., Iseki, E., ... McGeer, P.L., 2004. Expression of BRI, the normal precursor of the amyloid protein of familial British dementia, in human brain. *Acta neuropathologica* 107 (1), 53–58. <https://doi.org/10.1007/s00401-003-0783-1>.
- Ankarcrona, M., Winblad, B., Monteiro, C., Fearn, C., Powers, E.T., Johansson, J., ... Kelly, J.W., 2016. Current and future treatment of amyloid diseases. *J Intern Med* 280 (2), 177–202. <https://doi.org/10.1111/joim.12506>.
- Arosio, P., Michaels, T.C., Linse, S., Mansson, C., Emanuelsson, C., Presto, J., ... Knowles, T.P., 2016. Kinetic analysis reveals the diversity of microscopic mechanisms through which molecular chaperones suppress amyloid formation. *Nat Commun* 7, 10948. <https://doi.org/10.1038/ncomms10948>.
- Arvanitis, C.D., Askoxylakis, V., Guo, Y.T., Detta, M., Kloepper, J., Ferraro, G.B., ... Jain, R.K., 2018. Mechanisms of enhanced drug delivery in brain metastases with focused ultrasound-induced blood-tumor barrier disruption. *Proceedings of the National Academy of Sciences of the United States of America* 115 (37), E8717–E8726. <https://doi.org/10.1073/pnas.1807105115>.
- Baron, B.W., Pytel, P., 2017. Expression pattern of the BCL6 and ITM2B proteins in normal human brains and in Alzheimer disease. *Appl. Immunohistochem. Mol. Morphol.* 25 (7), 489–496. <https://doi.org/10.1097/PAI.0000000000000329>.
- Baseri, B., Choi, J.J., Tung, Y.S., Konofagou, E.E., 2010. Multi-modality safety assessment of blood-brain barrier opening using focused ultrasound and definity microbubbles: a short-term study. *Ultrasound Med. Biol.* 36 (9), 1445–1459. <https://doi.org/10.1016/j.ultrasmedbio.2010.06.005>.
- Baseri, B., Choi, J.J., Deffieux, T., Samiotaki, G., Tung, Y.S., Olumolade, O., ... Konofagou, E.E., 2012. Activation of signaling pathways following localized delivery of systemically administered neurotrophic factors across the blood-brain barrier using focused ultrasound and microbubbles. *Phys Med Biol* 57 (7), N65–81. <https://doi.org/10.1088/0031-9155/57/7/N65>.
- Branjevic, I., Steinbusch, H.W.M., Schmitz, C., Martinez-Martinez, P., Res, E.N., 2009. Delivery of peptide and protein drugs over the blood-brain barrier. *Prog. Neurobiol.* 87 (4), 212–251. <https://doi.org/10.1016/j.pneurobio.2008.12.002>.
- Burgess, A., Hynynen, K., 2014. Drug delivery across the blood-brain barrier using focused ultrasound. *Expert Opin. Drug Deliv.* 11 (5), 711–721. <https://doi.org/10.1517/17425247.2014.897693>.
- Cantlon, A., Frigerio, C.S., Freir, D.B., Boland, B., Jin, M., Walsh, D.M., 2015. The familial British dementia mutation promotes formation of neurotoxic cystine cross-linked amyloid Bri (ABri) oligomers. *J. Biol. Chem.* 290 (27), 16502–16516. <https://doi.org/10.1074/jbc.M115.652263>.
- Chen, G.F., Abelein, A., Nilsson, H.E., Leppert, A., Andrade-Talavera, Y., Tambaro, S., ... Johansson, J., 2017. Bri2 BRICHOS client specificity and chaperone activity are governed by assembly state. *Nat Commun* 8 <https://doi.org/10.1038/s41467-017-02056-4>. (doi:ARTN 2081).
- Chen, H., Chen, C.C., Acosta, C., Wu, S.Y., Sun, T., Konofagou, E.E., 2014. A new brain drug delivery strategy: focused ultrasound-enhanced intranasal drug delivery. *PLoS One* 9 (10), e108880. <https://doi.org/10.1371/journal.pone.0108880>.
- Choi, J.J., Pernot, M., Brown, T.R., Small, S.A., Konofagou, E.E., 2007a. Spatio-temporal analysis of molecular delivery through the blood-brain barrier using focused ultrasound. *Phys. Med. Biol.* 52 (18), 5509–5530. <https://doi.org/10.1088/0031-9155/52/18/004>.
- Choi, J.J., Pernot, M., Small, S.A., Konofagou, E.E., 2007b. Noninvasive, transcranial and localized opening of the blood-brain barrier using focused ultrasound in mice. *Ultrasound Med. Biol.* 33 (1), 95–104. <https://doi.org/10.1016/j.ultrasmedbio.2006.07.018>.
- Cohen, S.I.A., Arosio, P., Presto, J., Kurundenkandy, F.R., Biverstal, H., Dolfe, L., ... Linse, S., 2015. A molecular chaperone breaks the catalytic cycle that generates toxic Abeta oligomers. *Nature structural & molecular biology* 22 (3), 207–213. <https://doi.org/10.1038/nsmb.2971>.
- Downs, M.E., Buch, A., Sierra, C., Karakatsani, M.E., Teichert, T., Chen, S., ... Ferrera, V.P., 2015. Long-Term Safety of Repeated Blood-Brain Barrier Opening via Focused Ultrasound with Microbubbles in Non-Human Primates Performing a Cognitive Task. *PLoS one* 10 (5), e0125911. <https://doi.org/10.1371/journal.pone.0125911>.
- Feshitan, J.A., Chen, C.C., Kwan, J.J., Borden, M.A., 2009. Microbubble size isolation by differential centrifugation. *J. Colloid Interface Sci.* 329 (2), 316–324. <https://doi.org/10.1016/j.jcis.2008.09.066>.
- Finder, V.H., Glockshuber, R., 2007. Amyloid-beta aggregation. *Neurodegener. Dis.* 4 (1), 13–27. <https://doi.org/10.1159/000100355>.
- Glasser, S.W., Korfhagen, T.R., Bruno, M.D., Dey, C., Whitsett, J.A., 1990. Structure and expression of the pulmonary surfactant protein-Sp-C gene in the mouse. *J. Biol. Chem.* 265 (35), 21986–21991.
- Halliday, G., 2017. Pathology and hippocampal atrophy in Alzheimer's disease. *Lancet. Neurol.* 16 (11), 862–864. [https://doi.org/10.1016/S1474-4422\(17\)30343-5](https://doi.org/10.1016/S1474-4422(17)30343-5).
- Hardy, J., Selkoe, D.J., 2002. The amyloid hypothesis of Alzheimer's disease: progress and problems on the road to therapeutics. *Science* 297 (5580), 353–356. <https://doi.org/10.1126/science.1072994>.
- Hedlund, J., Johansson, J., Persson, B., 2009. BRICHOS - a superfamily of multidomain proteins with diverse functions. *BMC Res Notes* 2, 180. <https://doi.org/10.1186/1756-0500-2-180>.
- Hermansson, E., Schultz, S., Crowther, D., Linse, S., Winblad, B., Westermark, G., ... Presto, J., 2014. The chaperone domain BRICHOS prevents CNS toxicity of amyloid-beta peptide in *Drosophila melanogaster*. *Disease models & mechanisms* 7 (6), 659–665. <https://doi.org/10.1242/dmm.014787>.
- Hynynen, K., McDannold, N., Vykhotseva, N., Jolesz, F.A., 2001. Noninvasive MR imaging-guided focal opening of the blood-brain barrier in rabbits. *Radiology* 220 (3), 640–646. <https://doi.org/10.1148/radiol.2202001804>.
- Johansson, H., Nordling, K., Weaver, T.E., Johansson, J., 2006. The Brichos domain-containing C-terminal part of pro-surfactant protein C binds to an unfolded poly-Val transmembrane segment. *J. Biol. Chem.* 281 (30), 21032–21039. <https://doi.org/10.1074/jbc.M603001200>.
- Johansson, H., Eriksson, M., Nordling, K., Presto, J., Johansson, J., 2009. The Brichos domain of pro-surfactant protein C can hold and fold a transmembrane segment. *Protein Sci.* 18 (6), 1175–1182. <https://doi.org/10.1002/pro.123>.
- Knight, S.D., Presto, J., Linse, S., Johansson, J., 2013. The BRICHOS domain, amyloid fibril formation, and their relationship. *Biochemistry* 52 (43), 7523–7531. <https://doi.org/10.1021/bi400908x>.
- Konofagou, E.E., 2012. Optimization of the ultrasound-induced blood-brain barrier opening. *Theranostics* 2 (12), 1223–1237. <https://doi.org/10.7150/tno.5576>.
- Kronqvist, N., Sarr, M., Lindqvist, A., Nordling, K., Otkovs, M., Venturi, L., ... Johansson, J., 2017. Efficient protein production inspired by how spiders make silk. *Nat Commun* 8 <https://doi.org/10.1038/ncomms15504>. doi:ARTN 15504.
- Kurundenkandy, F.R., Zilberter, M., Biverstal, H., Presto, J., Honcharenko, D., Stromberg, R., ... Fisahn, A., 2014. Amyloid-beta-Induced Action Potential Desynchronization and Degradation of Hippocampal Gamma Oscillations Is Prevented by Interference with Peptide Conformation Change and Aggregation. *J Neurosci* 34 (34), 11416–11425. <https://doi.org/10.1523/Jneurosci.1195-14.2014>.
- Lashley, T., Revez, T., Plant, G., Bandopadhyay, R., Lees, A.J., Frangione, B., ... Holton, J.L., 2008. Expression of BRI2 mRNA and protein in normal human brain and familial British dementia: its relevance to the pathogenesis of disease. *Neuropathology and applied neurobiology* 34 (5), 492–505. <https://doi.org/10.1111/j.1365-2990.2008.00935.x>.
- Lipsman, N., Meng, Y., Bethune, A.J., Huang, Y.X., Lam, B., Masellis, M., ... Black, S.E., 2018. Blood-brain barrier opening in Alzheimer's disease using MR-guided focused ultrasound. *Nat Commun* 9 <https://doi.org/10.1038/s41467-018-04529-6>. doi:ARTN 2336.
- McDannold, N., Arvanitis, C.D., Vykhotseva, N., Livingstone, M.S., 2012. Temporary disruption of the blood-brain barrier by use of ultrasound and microbubbles: safety and efficacy evaluation in rhesus macaques. *Cancer Res.* 72 (14), 3652–3663. <https://doi.org/10.1158/0008-5472.CAN.12-0128>.
- Mikitsch, J.L., Chacko, A.M., 2014. Pathways for small molecule delivery to the central nervous system across the blood-brain barrier. *Perspect. Med. Chem.* 6, 11–24. <https://doi.org/10.4137/PMC.S13384>.
- Nisbet, R.M., Van der Jeugd, A., Leinenga, G., Evans, H.T., Janowicz, P.W., Gotz, J., 2017. Combined effects of scanning ultrasound and a tau-specific single chain antibody in a tau transgenic mouse model. *Brain* 140, 1220–1230. <https://doi.org/10.1093/brain/awx052>.
- Noege, L.M., Dunbar 3rd, A.E., Wert, S.E., Askin, F., Hamvas, A., Whitsett, J.A., 2001. A mutation in the surfactant protein C gene associated with familial interstitial lung disease. *N. Engl. J. Med.* 344 (8), 573–579. <https://doi.org/10.1056/NEJM20010223440805>.
- Noege, L.M., Dunbar 3rd, A.E., Wert, S., Askin, F., Hamvas, A., Whitsett, J.A., 2002. Mutations in the surfactant protein C gene associated with interstitial lung disease. *Chest* 121 (3 Suppl), 20S–21S. <https://doi.org/10.1378/chest.121.3.suppl.20s>.
- Olumolade, O.O., Wang, S., Samiotaki, G., Konofagou, E.E., 2016. Longitudinal motor and behavioral assessment of blood-brain barrier opening with transcranial focused ultrasound. *Ultrasound Med. Biol.* 42 (9), 2270–2282. <https://doi.org/10.1016/j.ultrasmedbio.2016.05.004>.
- Poska, H., Haslbeck, M., Kurundenkandy, F.R., Hermansson, E., Chen, G., Kostallas, G., ... Johansson, J., 2016. Dementia-related Bri2 BRICHOS is a versatile molecular chaperone that efficiently inhibits Abeta42 toxicity in *Drosophila*. *The Biochemical journal* 473 (20), 3683–3704. <https://doi.org/10.1042/BCJ20160277>.
- Sanchez-Pulido, L., Devos, D., Valencia, A., 2002. BRICHOS: a conserved domain in proteins associated with dementia, respiratory distress and cancer. *Trends Biochem. Sci.* 27 (7), 329–332.
- Schindelin, J., Arganda-Carreras, I., Frise, E., Kaynig, V., Longair, M., Pietzsch, T., ... Cardona, A., 2012. Fiji: an open-source platform for biological-image analysis. *Nat Methods* 9 (7), 676–682. <https://doi.org/10.1038/nmeth.2019>.
- Sierra, C., Acosta, C., Chen, C., Wu, S.Y., Karakatsani, M.E., Bernal, M., Konofagou, E.E., 2017. Lipid microbubbles as a vehicle for targeted drug delivery using focused ultrasound-induced blood-brain barrier opening. *J Cerebr Blood F Met* 37 (4), 1236–1250. <https://doi.org/10.1177/0271678X16652630>.
- Strazielle, N., Ghersi-Egea, J.F., 2016. Potential pathways for CNS drug delivery across the blood-cerebrospinal fluid barrier. *Curr. Pharm. Des.* 22 (35), 5463–5476.
- Tambaro, S., Galan-Acosta, L., Leppert, A., Chen, G., Biverstal, H., Presto, J., ... Johansson, J., 2019. Blood-brain and blood-cerebrospinal fluid passage of BRICHOS domains from two molecular chaperones in mice. *The Journal of biological chemistry* 294 (8), 2606–2615. <https://doi.org/10.1074/jbc.RA118.004538>.
- Tung, Y.S., Vlachos, F., Feshitan, J.A., Borden, M.A., Konofagou, E.E., 2011. The mechanism of interaction between focused ultrasound and microbubbles in blood-brain

- barrier opening in mice. *J. Acoust. Soc. Am.* 130 (5), 3059–3067. <https://doi.org/10.1121/1.3646905>.
- Ueno, M., Akiguchi, I., Hosokawa, M., Kotani, H., Kanenishi, K., Sakamoto, H., 2000. Blood-brain barrier permeability in the periventricular areas of the normal mouse brain. *Acta Neuropathol.* 99 (4), 385–392.
- Villasenor, R., Lampe, J., Schwanning, M., Collin, L., 2019. Intracellular transport and regulation of transcytosis across the blood-brain barrier. *Cell. Mol. Life Sci.* 76 (6), 1081–1092. <https://doi.org/10.1007/s00018-018-2982-x>.
- Vlachos, F., Tung, Y.S., Konofagou, E.E., 2010. Permeability assessment of the focused ultrasound-induced blood-brain barrier opening using dynamic contrast-enhanced MRI. *Phys. Med. Biol.* 55 (18), 5451–5466. <https://doi.org/10.1088/0031-9155/55/18/012>.
- Willander, H., Askarieh, G., Landreh, M., Westermark, P., Nordling, K., Keranen, H., ... Johansson, J., 2012. High-resolution structure of a BRICHOS domain and its implications for anti-amyloid chaperone activity on lung surfactant protein C. *Proceedings of the National Academy of Sciences of the United States of America* 109 (7), 2325–2329. <https://doi.org/10.1073/pnas.1114740109>.
- Winblad, B., Amouyel, P., Andrieu, S., Ballard, C., Brayne, C., Brodaty, H., ... Zetterberg, H., 2016. Defeating Alzheimer's disease and other dementias: a priority for European science and society. *Lancet Neurology* 15 (5), 455–532. [https://doi.org/10.1016/S1474-4422\(16\)00062-4](https://doi.org/10.1016/S1474-4422(16)00062-4).
- Wu, S.Y., Tung, Y.S., Marquet, F., Downs, M., Sanchez, C., Chen, C., ... Konofagou, E., 2014. Transcranial cavitation detection in primates during blood-brain barrier opening--a performance assessment study. *IEEE Trans Ultrason Ferroelectr Freq Control* 61 (6), 966–978. <https://doi.org/10.1109/TUFFC.2014.2992>.
- Zeisel, A., Munoz-Manchado, A.B., Codeluppi, S., Lonnerberg, P., La Manno, G., Jureus, A., ... Linnarsson, S., 2015. Cell types in the mouse cortex and hippocampus revealed by single-cell RNA-seq. *Science* 347 (6226), 1138–1142. <https://doi.org/10.1126/science.aaa1934>.